APPENDIX II.6

CHARACTERIZATION OF SPARSELY LONG CHAIN BRANCHED POLYCARBONATE BY A COMBINATION OF SOLUTION, RHEOLOGY AND SIMULATION TECHNIQUES

E.van Ruymbeke, A. Kaivez, A. Hagenaars, D. Daoust,
P. Godard, R. Keunings, C. Bailly

6.1 INTRODUCTION

It is well known that the presence of a small number of long chain branches, typically less than one per polymer chain, can significantly improve specific processability aspects of polymers, such as drawability, melt strength, etc..., without detrimental effects on mechanical properties. Sensitive and accurate methods to detect long chain branching (LCB) of sparsely branched polymers are thus very important, especially those providing information on the number and length of the branches as well as their distribution across the molar mass distribution (MMD).

In order to determine LCB content, several techniques are known [1-4]. The most direct ones are spectroscopic methods, in particular nuclear magnetic resonance (NMR). The current drawback of this technique is the limited branching length resolution. Branches longer than about eight carbons cannot be distinguished by the best

instruments [5-10], whereas branching length relevant for rheological properties is equal to at least twice the entanglement molecular weight, usually one order of magnitude higher. Rheology, on the other hand, is very sensitive to even minute levels of branching, but the rheological response alone is often ambiguous [2,4,10-13,]. Indeed, the rheological characteristics of a linear polymer with broad MMD and that of a long chain branched polymer can be quite similar [14]. Only a comparison of the experimental data with predictions of a quantitative model can eliminate the ambiguity if the true MMD is known [15]. Solution characterisation methods can provide unambiguous information on MMD and LCB when so-called coupled techniques are used, i.e. the simultaneous fractionation of the macromolecules by size exclusion chromatography (SEC) coupled viscometry and/or light scattering characterization of the fractionated species [3,9,10,16-21]. However, the sensitivity of coupled solution techniques to LCB is clearly limited. LCB can only be detected by a small modification of the coil size at same MW or retention time, as detected by intrinsic viscosity (*g'* factor) [2,22-24] or light scattering (*g* factor). The sensitivity of solution methods can be enhanced by a fractionation of the samples at the semi-preparative scale in order to concentrate the parts of the MMD with the highest branching content [15].

6.1.1 Solution characterization

The viscometric parameter characterizing LCB is $g' = ([\eta]_{br}/[\eta]_{lin})_M$, where $[\eta]_{br}$ and $[\eta]_{lin}$ are the intrinsic viscosities of respectively branched and linear polymers of the same molar mass M. The correlation of a global g' with an average LCB content has been attempted in a few publications for polycarbonate (PC) [22,24,25]. This approach mostly fails, mainly because of the lack of adequate models for the correlation. Better methods are based on the coupling of SEC with viscometry (SEC-IV), which allows "local" branching characterization from knowledge of g'_i for each chromatographic slice.

Because SEC-IV is an indirect technique, a procedure is required to transform *g'* into a branching density or overall number of branches. The only theoretical formulae relating the influence of chain architecture to solution properties have been developed by Zimm and Stockmayer [22]. They link the geometric structure factor *g* (defined as the ratio between the radii of gyration of the branched and linear polymers of the same molar mass respectively) with the number of branches per chain, for several architectures. These formulae are only valid in theta solvent. Moreover, a formula to transform *g'* into *g* is required. Although a power law is usually assumed for the transformation, the value of the exponent is ill-defined (reported values ranging from 0.5 to 1.5) [23,27-30]. In order to eliminate these two problems, some studies have been performed on model polymers with a known branching structure and content. Douglas and Freed [25] as well as Balke et al. [26] have proposed experimental formulae for monodisperse star polymers, which directly link *g'* to the number of arms.

We have recently established a relationship between *g'* and the number of long chain branches of a polydisperse polymer for a model system consisting of polydisperse linear polystyrene blended with a small and known fraction of monodisperse 3-arm stars [31]. We have shown that semi-quantitative detection of the branched fraction can be obtained from the Mark-Houwink plot. The link between local g_i' and a long chain branching index (LCBI) expressed as the number of long chain branches per chain has been established [32]:
$g_i' > 0,92$: quasi linear chains (LCBI≤ 0.25)
$0,85 \leq g_i' \leq 0,92$: slightly branched chains (0.3≤LCBI≤ 0.5)
$g_i' < 0,85$: pure 3-arms stars (LCBI=1)
In this work, we try to extend these observations to randomly branched polycarbonate.

6.1.2 Rheological characterization

Many studies [2,4,10-13,15] have shown that the presence of LCB in a well-entangled polymer melt has a dominant influence on linear viscoelasticity. The relaxation of a long chain branched polymer is in most cases much slower than the relaxation of a linear polymer with the same MMD. Following tube theory, this is understood by a completely different balance between reptation and fluctuations relaxation processes for the two architectures. Tube-based models predicting linear viscoelasticity for linear polymers have reached an excellent level of quantitative agreement with experiments [33-36]. Therefore, discrepancies between the experimental relaxation of a given long chain branched sample and its predicted relaxation, calculated *assuming that the polymer is linear,* can give important qualitative information about the presence of LCB [15]. The confident use of such a model requires an excellent knowledge of the true MMD. On the other hand, no quantitative reptation models exists for complex polymers characterized by polydispersity in molar mass and architecture, including sparsely branched polymers such as the ones used in this study. Hence, direct quantification of LCB based on reptation models remains elusive at the moment.

6.1.3 This work

The overall objective of this paper is to show that the combined use of fractionation, solution characterization, rheological measurements and modelling can provide unambiguous and highly sensitive information on the branching structure of a model long chain branched polymer with very low level of branching (less than 1 branching point per 10 chains on average). The model polymer used for this study is bisphenol A polycarbonate (PC) obtained by melt transesterification from bisphenol A and diphenyl carbonate [37]. Branches result from a side-reaction leading to the random incorporation of trifunctional monomer units. The choice for this system is based on two main considerations :

(i) A method for continuous preparative fractionation (CPF) has recently been developed for PC [37]. Through this technique,

preparative size fractions of relatively narrow dispersity (polydispersity index around 1.5) can be obtained in a short time with limited use of solvent. For linear PC, the CPF method fractionates according to molar mass (MM) only [38]. For sparsely branched PC, this is also predominantly the case because, at a very low level of branching, solution properties are only marginally perturbed with respect to the linear polymer. It is thus possible to confirm and refine results obtained for broad, unfractionated samples, by analyses of narrow fractions.
(ii) Because melt transesterification of PC is an equilibrated reaction, the resulting distribution for the linear polymer is of the "most probable" or "Flory" type [39]. Moreover, branching of this system can be considered as a random process. Therefore, a Monte-Carlo simulation method can be used to predict the statistical molecular structure of melt branched PC [40-42].

The paper is divided in four sections following this Introduction. In Section 2, we recall the main features of our new reptation model, which will be used to highlight LCB in some of the PC samples, and we present a Monte-Carlo simulation approach, which allows an explicit and quantitative description of the chain architectures present in the sample. Section 3 is devoted to a description of the experimental techniques used and samples tested. In Section 4, we present and discuss the results of the solution and rheological analyses and compare them to the output of the Monte-Carlo simulations. Conclusions are drawn in Section 5.

6.2. THEORY AND SIMULATIONS

6.2.1 Rheological model

For the rheology predictions, we have used a new model based on tube theory, which has been recently published in [43]. Starting from a classical description of reptation, fluctuations and constraint release processes, the model is able to predict the linear viscoelastic behaviour of mixtures of (asymmetric) star and linear polymers from knowledge

of their structure. As our aim is to highlight a discrepancy between measured dynamic moduli and predictions based on the assumption of linearity of the molecules, we can here limit the application of the model to linear polydisperse polymers. A complete description has been published in [43].

According to tube theory, each entangled molecule in a polymer melt can be pictured as if it were confined by a virtual tube [44,45]. The tube represents the entanglement constraints on the observed molecule by the surrounding chains. In order to relax after a deformation, a test molecule has to move out of its original tube. In this way, it looses the memory of the orientation and recovers an equilibrium coil conformation. This memory loss is described by the relaxation function $F(t)$, defined as the unrelaxed fraction of the polymer melt at time t. In our model, it is taken as the weighted sum of the probabilities that any chain segment is not yet relaxed at the observed time t:

$$F(t)=\sum_i \varphi_i \int_0^1 \left(p_{rept}(x_i,t)\cdot p_{fluc}(x_i,t)\cdot p_{envir}(x_i,t)\right) dx_i \,, \qquad (1)$$

where x_i is a parameter describing the position of a primitive chain segment along a chain "i" ; x_i goes from 0 at the end of a chain to 1 at the center; $\varphi(i)$ represents the volumetric fraction of chain "i", and $p(x_i,t)$ represents the survival probability of segment x_i, at time t. Each segment can relax in three different ways, which will be explained below: by reptation, by fluctuations, or by the environment. The relaxation modulus $G(t)$, which is directly linked to the experimentally accessible dynamic modulus through mathematical transformations, is the product of $F(t)$ and of the plateau modulus G_N^0. In order to obtain $F(t)$, we use a time-marching algorithm, which calculates, at each time step, the polymer fraction already relaxed by reptation or by fluctuations, called $\Phi(t)$. This is essential because the relaxed fraction can in some cases speed up the characteristic relaxation times. In the specific case of polydisperse linear chains, $\Phi(t)$ influences the characteristic fluctuations relaxation time but not the reptation time. This difference is based on the "Graessley criterion" and is explained

in detail in [43,46]. Because of this feedback effect of the relaxed part on relaxation times, no analytic solution can be found for the relaxation function of polydisperse linear polymers.

The term p_{rept} in Eq.(1) represents the probability that a given tube segment located at x_i is not relaxed by reptation at time t. This is the main relaxation process of a linear chain. Based on the work of Doi and Edwards [45], we can calculate the survival probability by reptation of a given tube segment, after a time interval Δt:

$$p_{rept}(x_i, \Delta t) = \sum_{p\ odd} \frac{4}{p\pi} \sin\left(\frac{p\pi x_i}{2}\right) \exp\left(\frac{-p^2 \Delta t}{\tau_{rept}(M)}\right), \qquad (2)$$

where τ_{rept} is the reptation time of the observed molecule. For linear polydisperse chains, τ_{rept} is only a function of molar mass and of a segmental relaxation time τ_e :

$$\tau_{rept}(M) = 3\ \tau_e \left(\frac{M}{M_e}\right)^3, \qquad (3)$$

We use a time marching algorithm to calculate survival probabilities along a discretized time axis

$$p_{rept}(x_i, t_k) = p_{rept}(x_i, t_{k-1}) \cdot p_{rept}(x_i, [t_{k-1}, t_k]). \quad (4)$$

The survival probability after reptation, at time t_k is the product of the survival probability at time t_{k-1} and the survival probability during an interval Δt comprised between t_{k-1} and t_k. The latter can be calculated from Eq. (2).

The term p_{fluc} in Eq. (1) determines the probability that an initial tube segment is not yet relaxed by tube length fluctuations. This is the main relaxation process of a branched molecule, but it also happens during the relaxation of a linear chain. This relaxation comes from the fact the length of a chain fluctuates around an equilibrium value. Fluctuations shortening the occupied tube length will relax part of the orientation. The equilibrium length depends on the relaxed fraction:

$$L_{eq}(t) = L_{eq,0}.\left(\Phi(t)\right)^{\alpha/2} \qquad (5)$$

where L_{eq0} represents the equilibrium length at time 0 and α is the dilution exponent [47-49]. The time for a segment to relax by fluctuations increases exponentially with a fluctuations potential that results from the balance of the chain entropic spring force and of the tube constraint [50]. Using the idea of dynamic dilution [51,52], it is possible to calculate the dependence of the potential on the fluctuations depth x_i :

$$\frac{\partial \ln \tau_{fluc}(x_i)}{\partial x_i} = \frac{\partial\left(U(x_i)/kT\right)}{\partial x_i} = 3 \cdot Z_i \cdot x_i \cdot \Phi_{active}(t, x_i)^{\alpha}, \qquad (6)$$

where Φ_{active} is the unrelaxed fraction active for the fluctuations process at x_i and time t, and Z_i is the number of entanglements of chain "i". Using the Graessley criterion [46], we can show that, for polydisperse linear molecules, $\Phi_{active}(t,x_i)$ is affected by fluctuations but not by reptation. For segments close to the chain end, fluctuations are not controlled by the potential but by unconstrained Rouse motions of the chain end:

$$\tau_{early}(x_i, t_k) = \frac{9\pi^3}{16} \cdot \left(\frac{M_a \cdot \phi_{rept}(t_k)^{\alpha}}{M_{e,0}} \right)^2 \cdot \tau_{R,chain} \cdot x_i^{\,4}. \qquad (7)$$

The transition between these "early" fluctuations and those controlled by the potential occurs at a transition segment where the potential is

equal to kT. The fluctuations survival probability between t_k and $t_k+\Delta t$ can be calculated from knowledge of the fluctuations time $\tau_{fluc}(x_i,t_k)$:

$$p_{survival}(x_i,\Delta t) = \exp\frac{-(\Delta t)}{\tau_{fluc}(x_i,t_k)}. \qquad (8)$$

The fluctuations survival probability can be updated at increasing times in the same way as the reptation process (Eq. 4 with p_{fluc} replacing p_{rept}).

The term p_{envir} in Eq. (1) describes the probability that the test segment is not relaxed by the relaxation of the surrounding molecules. This describes a thermal constraint release mechanism, which is a generalization of double reptation ideas. It is convenient and reasonably accurate to consider that the probability to lose an entanglement in this way is identical for all the segments in the polymer melt. Therefore p_{envir} is equal to the probability that an entanglement taken at random in the polymer is still oriented. The environment survival probability is a conditional probability applied to a segment, which is not relaxed by reptation nor by fluctuations. That implies that all the segments between the center of any molecule k and a fractional distance x_{k_trans} equivalent (potential-wise) to the test segment x_i, are also not relaxed by fluctuations. Therefore, the general expression of the environment survival probability can be described by the following equation:

$$p_{envir}(x_i,t) = \left(\sum_k \varphi_k \cdot \left[\int_0^{x_{k,trans}} p_{rept}(x_k,t)\; p_{fluc}(x_k,t)\; dx_k + \int_{x_{k,trans}}^{1} p_{rept}(x_k,t)\; dx_k \right] \right)^{\alpha}. \qquad (9)$$

In the model, only three materials parameters are needed: the plateau modulus G_N^0, the Rouse time of a segment, τ_e, and the molecular weight between two entanglements, M_e. Theoretically, G_N^0 and M_e are

linked [53] but in practice, it is necessary to slightly relax this restriction and treat the two parameters as independent (within reasonable bounds). The dilution exponent α can be considered as an additional fitting parameter within strict bounds. We have fixed the value of α at 1.2, which is consistent with literature [47-49].

The model is implemented in MatLab® as described in [43].

6.2.2 Monte-Carlo simulation

In order to approach the branching distribution of the investigated melt-polymerized samples from a theoretical standpoint, we have developed a simulation model based on a random sampling technique, also called Monte Carlo simulation. Three types of polymer building blocks must be considered: bifonctional units, which are the most common, trifonctional units, which represent the branching points, and monofunctional units, representing the terminal groups. For chemical reasons, bifunctional and trifunctional units are distributed randomly along the chains, i.e. the probability that any monomeric unit carries a branching point is independent of the status of other units on the same chain or others [37,40-42]. Terminal units are by definition located at a chain extremity. The number of linear, branching and terminal building blocks, respectively called *L*, *B* and *X*, can be calculated from the number average molecular weight M_n, the branching density ρ (the fraction of branching units) determined by NMR analysis, and an arbitrary total number *M* of building blocks used for the simulation:

$$B = \rho . M, \tag{10}$$

$$X = ((2+\rho)/M_n) . M, \tag{11}$$

$$L = M-B-X \tag{12}$$

Chains are constructed by picking up building blocks at random in a box containing the right numbers B, L and X of corresponding units. The starting point for the construction of any molecule has to be a

terminal group picked up from the same box. One additional terminal unit is enough for closure a linear chain, but a branched molecule requires additional terminal groups (one per branching point). When a branching monomer is taken from the box, we have to consider the construction of each of the two arms one after the other. A molecule is complete when all its arms are closed by a terminal group. Branching densities for the investigated systems are very small (between 1 and 3 10^{-3}; see Experimental Section). Therefore, we have only considered branched molecules up to a third generation tree architecture, as depicted in Figure 1.

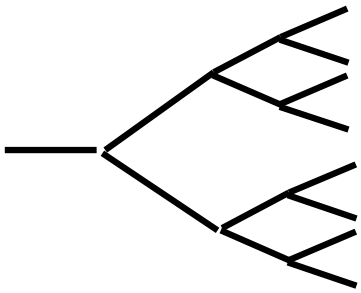

Fig. 1: Construction of the molecules from a terminal group, by considering a three-generations tree architecture.

The exhaustive information concerning the simulated molecules has been stocked in a large matrix, each line of which represents a specific molecule, and each of the 15 columns is associated with a specific arm represented in Figure 1. So, we know exactly the architecture of each molecule, and different statistical tests can easily be performed. In particular, we are interested to know the volumetric fraction of linear, star or higher branched molecules as a function of their molecular weight, i.e. the MMD of certain types of architecture.

The simulation procedure has been implemented in MatLab®.

6.3 EXPERIMENTAL SECTION

6.3.1 Materials

The solvent used for SEC was methylene chloride (HPLC grade from Acros).

Anionic polystyrene standards were used in order to construct the polystyrene and universal calibrations. Standards of molar mass (MM) 96400, 37900, 18100, 9100 and 870 g/mol were supplied by Tosoh, Japan. Standards of MM 460000, 156000, 76600, 28500, 22000, 11600, 7000, 5000, 3250 and 1680 g/mol were supplied by Polymer Laboratories, the Netherlands. A standard of MM 30000 g/mol was supplied by Pressure Chemicals USA.

In order to establish the viscosity law of linear PC and the "PC-specific" calibration, a broad linear PC sample (Lexan 130 from GE Plastics, obtained by interfacial synthesis) was used. Branched PC samples, called PC1 and PC2 and a linear PC reference, called PCL were synthesised by a melt transesterification process and fractionated by the continuous polymer fractionation method as described in [ ]. The fractions are denoted PCxFy, with x a reference to the original sample (L, 1 or 2) and y a reference to the fraction. Molar mass distributions are shown in Fig. 2 and average molecular weights are described in Table 1.

The average number of branching points in PC2 as determined by NMR and used for the Monte-Carlo simulation is 0.107 branching points per chain on average, which corresponds to a branching probability or density of $2.955\ 10^{-3}$ (that is the probability that a given monomer unit is branched along the chain). For PC1, the average number of branching points per chains is equal to 0.04 and its branching probability is $1.068\ 10^{-3}$. Several blends of PC2F1 and PC2F4 were also realised.

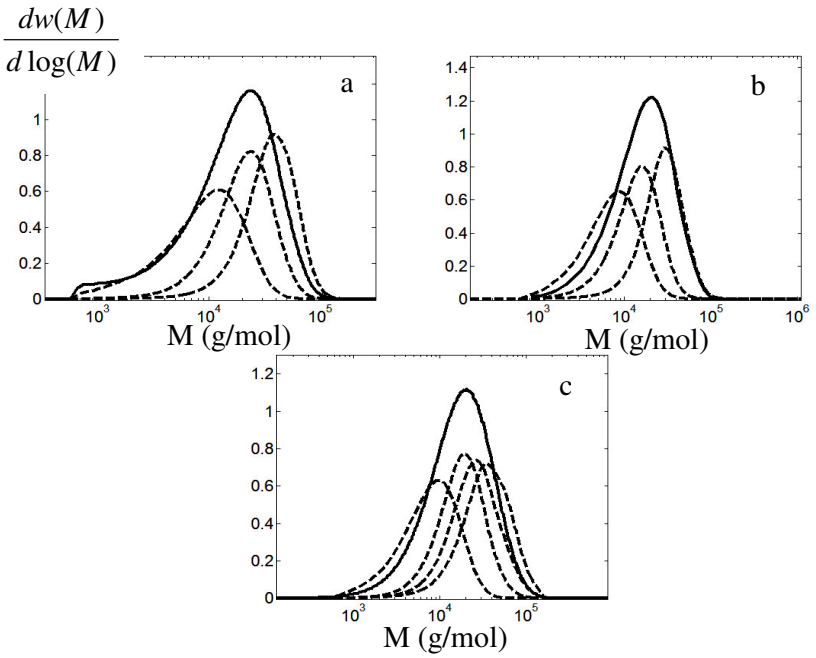

Figure 2: Molar masses distribution of a) PCL, b) PC1, c) PC2 and fractions of them (see Table 1).

Table 1: Average molar masses of PCL, PC1, PC2 and their fractions

	Mw (g/mol)	Mn (g/mol)	Ip = Mw/Mn
PCL	22700	9600	2.35
PCLF1	11300	5500	2.05
PCLF2	23200	15300	1.51
PCLF3	39000	28100	1.39
PC1	20500	9500	2.16
PC1F1	8700	5100	1.72
PC1F2	15900	10400	1.53
PC1F3	30900	21200	1.46
PC2	22400	9400	2.37
PC2F1	9500	5300	1.8
PC2F2	20700	13300	1.55
PC2F3	30100	18300	1.65
PC2F4	40600	24300	1.67

6.3.2 SEC-IV Chromatography

SEC – IV experiments were performed on a GPCV-2000 instrument from Waters. The solvent was methylene chloride, the flow rate, 1 ml/min, the temperature, 30°C, and the injection loop volume, 215.5µl. The columns were three PL gel columns from Polymer Laboratories (pore sizes : 100, 1000 and 10 000 Å). A differential refractometer was used as detector and calibrated for each polymer following a procedure described in a previous paper [54]. An interdetector delay of 0.057 min was determined following a procedure described in [55]. Data were acquired with the Alliance GPCV 2000 software from Waters at an acquisition rate of 5 pts/s. The data were processed using procedures developed in our laboratory using the IGOR software from Wavemetrics. In order to determine the molar mass distribution of branched PC, the evolution of intrinsic viscosity with retention time was approximated by a third order polynomial. This approximation was not used for the determination of viscosity laws and branching parameters, for which only slices with both significant signals were taken into account. In order to check for the composition of the blends of two fractions, the refractometer chromatograms were decomposed into the weighted sums of the two fractions analysed alone.

When analysing PC by SEC-viscometry, the applicability of universal calibration can sometimes be questioned. It does not represent any problem for sufficiently high molar masses, but the lower MM validity limit is not clearly defined [26,56], as well for universal calibration as for a linear viscosity law [57,58]. Therefore, the best calibrations for PC would be obtained by using some PC oligomers in the low molar mass region [59]. However, it is difficult to appropriately detect oligomers with the viscometer and to include them in the universal calibration. Moreover, long chain branching is scarcely expected to appear in the very low MM part of the distribution. Therefore, in this work, oligomer synthesis and fractionation were avoided and universal as well as PC specific calibrations were constructed using polystyrene standards and a broad linear PC. Moreover, we tried to characterize

branching only from the measured intrinsic viscosity at each retention time, without any calibration.

6.3.3 Rheological measurements

For rheological measurements, PC samples in powder form were pre-dried at 120°C overnight and subsequently pressed into compact circular pellets (10 mm diameter, 2 mm thickness) at room temperature using a hydraulic press. The pellets were then again dried under vacuum at 120°C overnight, prior to measurements.

Dynamic storage and loss moduli, G'(ω) and G"(ω), were determined with a strain-controlled ARES rheometer from Rheometrics in dynamic mode with a parallel-plate configuration at temperatures ranging from 160°C to 220°C. Linearity of the viscoelastic regime was checked with the help of a strain sweep. In order to conserve quantities of the fractionated samples, plates with a diameter of 8 mm were used. The angular frequency sweep interval was 10^{-1} to 5.10^{2} rad/sec, with a strain amplitude of 15%. All measurements were performed under dry nitrogen atmosphere. Master curves (reference temperature 200°C) were constructed by applying the Time-Temperature Superposition (TTS) principle with both horizontal and vertical shifts [60].

6.4 RESULTS

6.4.1 Solution characterisation

A. Global characterization

The best method to obtain a global index for long chain branching is to determine the branching parameter *g'*. To this end, a mean intrinsic viscosity must be obtained for each sample. Several possibilities exist for calculating these average values:

$$[\eta]_w = \frac{\sum c_i [\eta]_i}{\sum c_i}, \quad (13)$$

$$[\eta]_g = \frac{\sum \eta_{spec,i}}{\sum c_i}, \quad (14)$$

$$g'_w = \frac{\sum c_i g'_i}{\sum c_i}, \quad (15)$$

$$g'_g = \frac{\sum \eta_{spec,i}}{\sum c_i K M_i^{\alpha}}, \quad (16)$$

where c_i is the concentration of the ith slice, directly obtained from the refractometer chromatogram, $\eta_{spec,i}$ is the specific viscosity of the ith slice, directly obtained from the viscometer chromatogram, $[\eta]_i = \frac{\eta_{spec,i}}{c_i}$ is the intrinsic viscosity of the ith slice, M_i is the real molar mass of the ith slice, obtained from $[\eta]_i$ and the universal calibration, K and α are the Mark-Houwink coefficients [32] for linear polycarbonate, and

$$g'_i = \frac{[\eta]_i}{K M_i^{\alpha}} = \left(\frac{[\eta]_{br,i}}{[\eta]_{lin,i}} \right)_M , \quad (17)$$

is the branching coefficient of the ith slice.It should be noted that $[\eta]_w$ and $[\eta]_g$ represent the same macromolecular property: the intrinsic viscosity of the sample that could be measured with an 'off line' viscometer. However, $[\eta]_g$ is only based on the 2 chromatograms, whereas $[\eta]_w$ requires their slice per slice division. The same kind of nuance appears in the calculations of g'_w and g'_g.

The potential problem of all these global characteristics, except $[\eta]_g$, is that the molar mass of each slice must be calculated by universal calibration. Therefore, a polynomial fit of the intrinsic viscosity is necessary before applying this calibration, to eliminate meaningless values of $[\eta]$ at the peak feet. As already observed, the higher

retention time limit for evaluation of this polynomial is taken quite far from the peak foot, and low molar masses values obtained by this procedure can lack reproducibility. In order to get around this problem, another mean branching factor g'_{HV} has been calculated, based on the measured intrinsic viscosity of the branched polymer and of the intrinsic viscosity of linear PC:

$$g'_{HV,w} = \sum \frac{c_i g'_{HV,i}}{c_i}, \tag{18}$$

with :

$$g'_{HV,i} = \left(\frac{[\eta]_{br,i}}{[\eta]_{lin,i}} \right)_{HV} . \tag{19}$$

It is indicated by the subscript HV to denote that the intrinsic viscosity of each slice has been divided by the intrinsic viscosity of a linear polymer having the same hydrodynamic volume (thus retention time) as the branched polymers, and not the same molar mass, as in the usual *g'*. For determining $g'_{HV,w}$, the measured $[\eta]_i$ (*RT*) or their polynomial approximation can be used. A representative selection of the different results is shown in Table 2.

Table 2: Intrinsic viscosity and branching parameters of the PC samples and their fractions.

	$[\eta]_\omega$ (dl/g)	$[\eta]_g$ (dl/g)	g'_g	g'_ω	$g'_{HV,\omega}$ (no fit)	$g'_{HV,\omega}$ (fit) log[η] (RT))
PC1	1.13	1.18	0.89	0.88	0.92	0.92
PC1F1	0.66	0.65	0.87	0.87	0.80	0.91
PC1F2	0.99	0.97	0.89	0.89	0.88	0.93
PC1F3	1.59	1.60	0.95	0.94	0.97	0.96
PC2	1.18	1.19	0.91	0.91	1.01	0.94
PC2F1	0.71	0.71	0.91	0.90	0.93	0.94
PC2F2	1.14	1.13	0.86	0.87	0.91	0.92
PC2F3	1.42	1.43	0.90	0.90	0.94	0.94
PC2F4	1.75	1.74	0.85	0.90	0.92	0.93

Expectedly, the reproducibility for the low MM fractions is low, as illustrated by the difference between $g'_{HV,w}$ of PC1F1 with or without polynomial approximation of log[η](RT).

B. Local branching characterisation of the fractions

As the branching parameters only slightly differ from one fraction to another, it is difficult to classify these fractions according to their branching content and thus to locate the branched fractions into the complete samples PC1 or PC2. A more local branching characterization is thus necessary. First, we have analysed the fractions. Their main advantage is that both low MM and high MM parts of the distribution can be analysed at a much higher concentration than in the original polymer [15]. In a next step, several blends of fractions were analysed before finally going to the unfractionated samples.

The first polymer characteristic that can indicate the presence of long chain branching is the evolution of intrinsic viscosity with retention time. It is presented in Fig. 3 for all the PC2 fractions (i.e. the sample containing the highest level of branching units) together with a fitted $log[\eta](RT)$ for linear PC. The Figure shows a growing gap between the analysed fractions and linear PC for short retention times, thus mainly for PC2F3 and PC2F4. This seems to indicate the presence of long chain branching on high molar mass chains. This is confirmed by Fig. 4, which compares the viscosity laws of the fractions and of the linear PC. The disconnection between branched and linear PC is located around 40 000 g/mol.

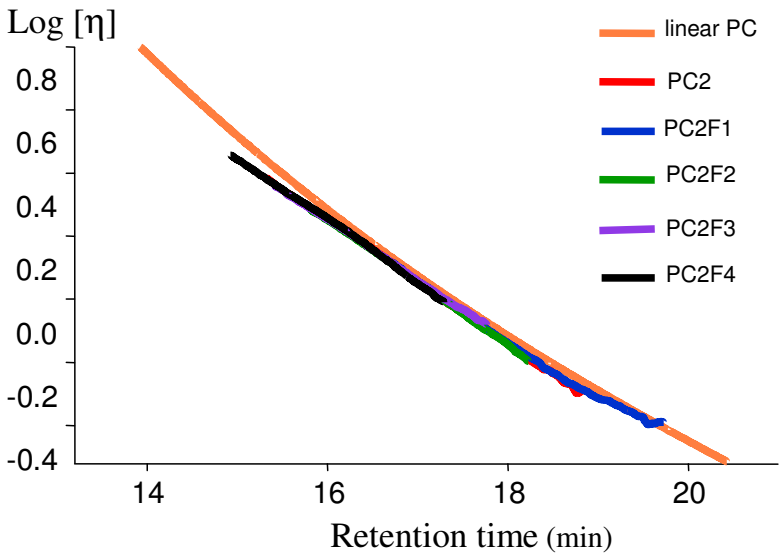

Figure 3: Evolution of intrinsic viscosity with retention time of PC2 and its fractions.

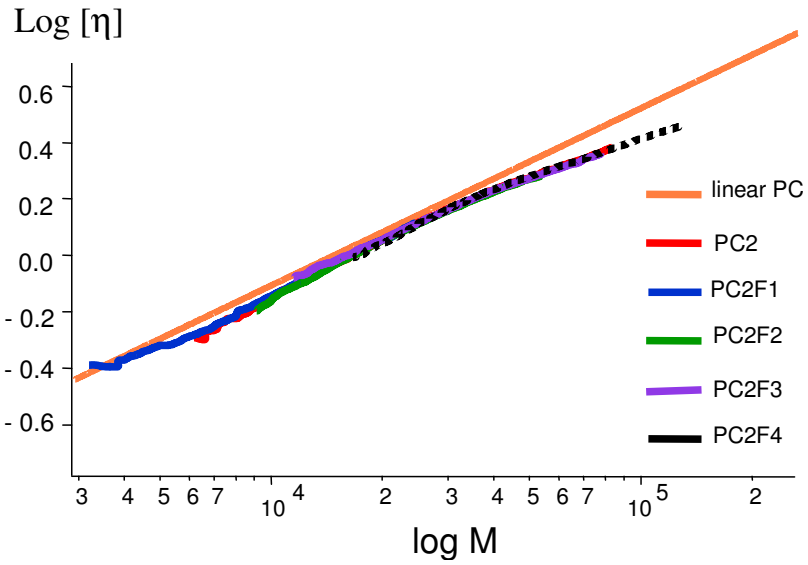

Figure 4:Viscosity law of PC2 and its fractions.

In order to quantify this long chain branching, slice by slice branching factors have been calculated. They have been determined by two different ways: $g'_{HV,i}$ and g'_i.
$g'_{HV,i}$ is the more easy to determine. It just needs a preliminary injection of a linear polymer in the same retention time range in order to know $[\eta]_{lin,i}$ at each retention time. No calibration has been used. Evolution of $g'_{HV,i}$ with retention time is presented in Fig. 5 for PC2 fractions.

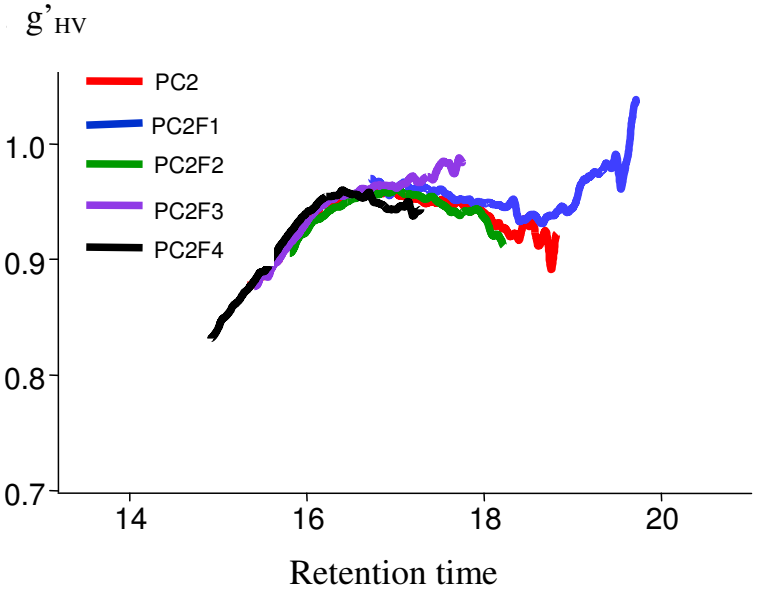

Figure 5: Evolution of g'_{HV} vs. the retention time of PC2 and its fractions.

Figure 6 presents the evolution of g'_i (Eq. 17) vs. molar mass for al PC fractions. This parameter is more complicated to determine and less accurate than $g'_{HV,i}$ since g'_i will be sensitive to calibration errors for the branched polymer, which is not the case g'_{HVi} as readily understood from a comparison of Eqs (17) and (19). However, it is necessary to calculate g'_i if we want to obtain the corresponding

geometric structure factor g_i in order to determine a number of branches, for example by using a Zimm and Stockmayer formula [22].

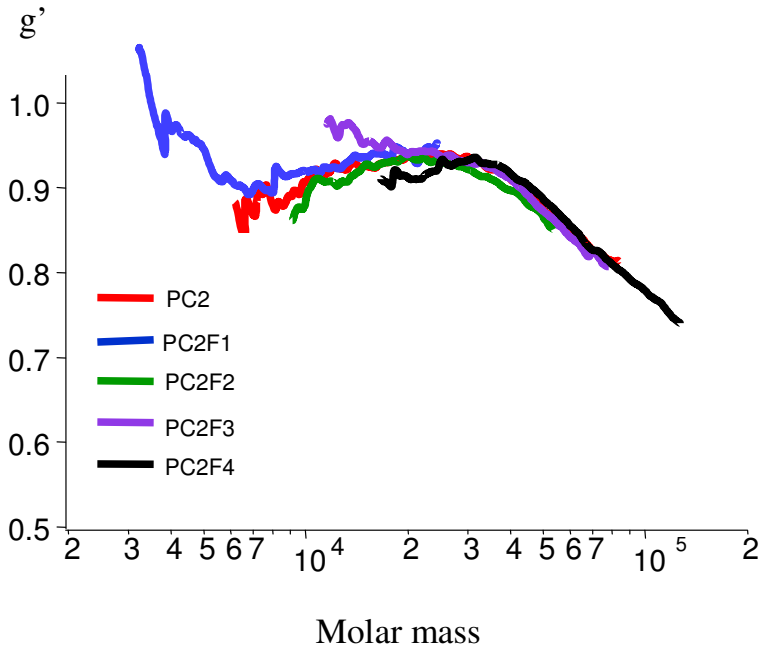

Fig. 6: Evolution of g' vs. the molar mass of PC2 and its fractions.

Comparing Figures 5 and 6, we observe that $g'_{HV,i}$ is always higher than g'_i. This is expected as long chain branching decreases hydrodynamic volume, thus increases retention time compared to a linear polymer of the same molar mass. Therefore, g'_{HV} divides $[\eta]_{br}$ by the intrinsic viscosity of a linear polymer of lower molar mass than g' does and is by consequence higher. We indicate in Figures 5 and 6 the highest and the lowest values obtained in several replicated analyses of each fraction. It can be seen that the reproducibility at low molar mass is very poor and that trying to obtain branching information about these fractions by SEC- IV cannot be achieved. However, for molar masses higher than 30 000 g/mol, (retention times

of 16.5 min or less), the data spread is small. The decrease of the branching index is observed at 40 000 g/mol for g'_i and 16 min for $g'_{HV,i}$. The value of g' at this molar mass is 0,92. This corresponds to the transition from quasi-linear polymer to slightly branched polymer in the classification established for polystyrene blends, as explained in the Introduction [31].

The same procedure was followed to analyse PC1 fractions. The evolution of $g'_{HV,i}$ together with the chromatograms of the different fractions, is presented in Fig. 7.

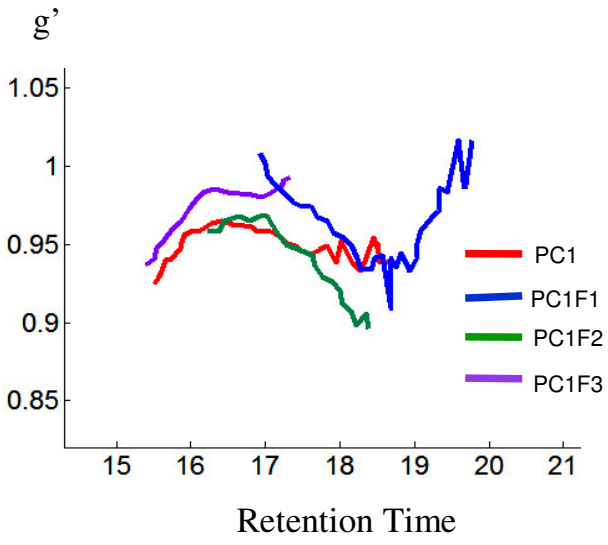

Figure 7: Evolution of g' vs. with retention time of PC1 and its fractions.

Even if a small decrease is observed at 16.5 min, it is difficult to assess if this decrease is significant enough to be attributed to branching. Obviously, the branching level of PC1 is below the detection limit of the solution characterization method.

C. Fractions blends and unfractionated samples

In order to analyse the detection limit of the branching index method, several blends of the two extreme PC2 fractions PC2F1 and PC2F4 were realised with weight ratios ranging from approximately 25 F1/75 F4 to 75 F1/25 F4 analysed in the same way as above. For all the blends, evolution of intrinsic viscosity at low retention superimposes with the one observed for PC2F4 alone. The conclusion about branching detection remains thus unchanged: even when the high molar mass fraction is present as 25% of the total, the decrease of g'_{HV} at retention times shorter than 16 min and of g' at molar masses higher than 40 000 g/mol are still observable and unchanged.

The evolution of intrinsic viscosity vs. retention time, the viscosity law and the evolution of the branching parameters g'_{HV} and g' for unfractionated PC2 are presented with those of the fractions in Figures 5 to 7. As indicated above, results for PC1 are below detection limit. In all the Figures, data located near the peak foot have been removed because of excessive noise. The results obtained for unfractionated PC2 are in good agreement with those of the fractions. On Figures 5 and 6, the reduction of g'_{HV} and g' can be observed, exactly as for PC2F4. However, the number of significant slices which showing this decrease is quite small, and the presence of long chain branching would have been difficult to ensure without the results obtained for the fractions.

6.4.2 Rheological results

We have first calibrated our model on the broad linear polydisperse sample PCL, and tested the calibration on its three fractions. Molecular characteristics of the samples are described in Table 1. Next, we have predicted the linear viscoelastic properties of the two sparsely branched samples PC1 and PC2. The model of course assumes that they are linear. The MMD of the samples obtained by universal calibration is used as input of the model. We have finally compared predictions and experimental data: if rheology is sensitive

enough to detect low levels of LCB, a discrepancy should appear. In Fig. 8, predicted and experimental data for the linear PC are compared. Only the terminal region is relevant for testing molecular architecture. The parameters we have used to fit PCL and to predict its fractions are 3.10^{-4} for τ_e, 1.5 MPa for G_N^0 and 2500 g/mol for M_e [61,62].

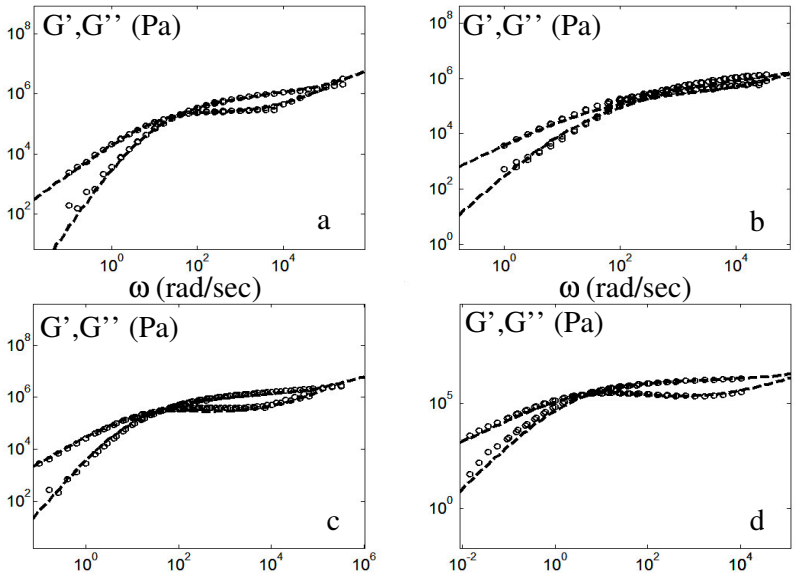

Figure 8: Comparison between experimental (ooo) and theoretical (--) storage and loss moduli for a) PCL, b) PCLF1, c) PCLF2, d) PCLF3.

The results are in very good agreement for the four tested samples. The apparent slight discrepancy observed for the lowest fraction (Fig. 8b) is in fact due to a partial overlap of the terminal and the Rouse relaxations in the terminal zone.

In the next step, we have used the same parameters to predict the linear viscoelasticity of the branched sample PC2 and its fractions, as shown in Fig. 9.

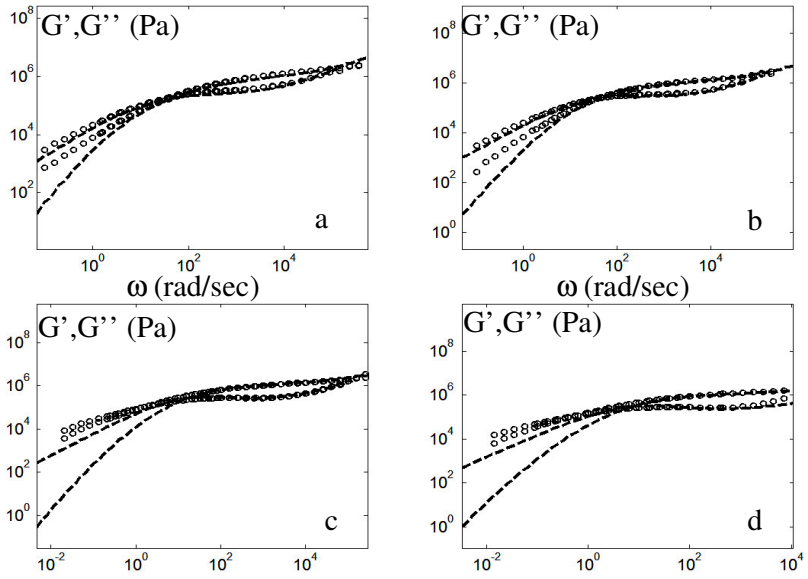

Figure 9: Comparison between experimental (ooo) and theoretical (--) storage and loss moduli for a) PC2, b) PC2F2, c) PC2F3, d) PC2F4.

The storage and the loss moduli predictions for PC2 and its fractions do not show quantitative agreement with the experimental data in the relevant terminal region. The discrepancy increases for the highest fractions, which means that these fractions seem more branched than the lowest molar mass fraction or the total sample. These results confirm that the rheological response of an entangled polymer is very sensitive to the presence of long chain branching when the obscuring influence of the MMD can be removed, in this case, through the use of a quantitative model. The rheology-based method is clearly more sensitive than the solution method since LCB was only

unambiguously detected for the highest fraction PC2F4 while it is clearly observed here on all fractions and the unfractionated sample.

In the same way, we have analysed the very low LCB sample PC1 and its fractions. The results are presented in Figure 10.

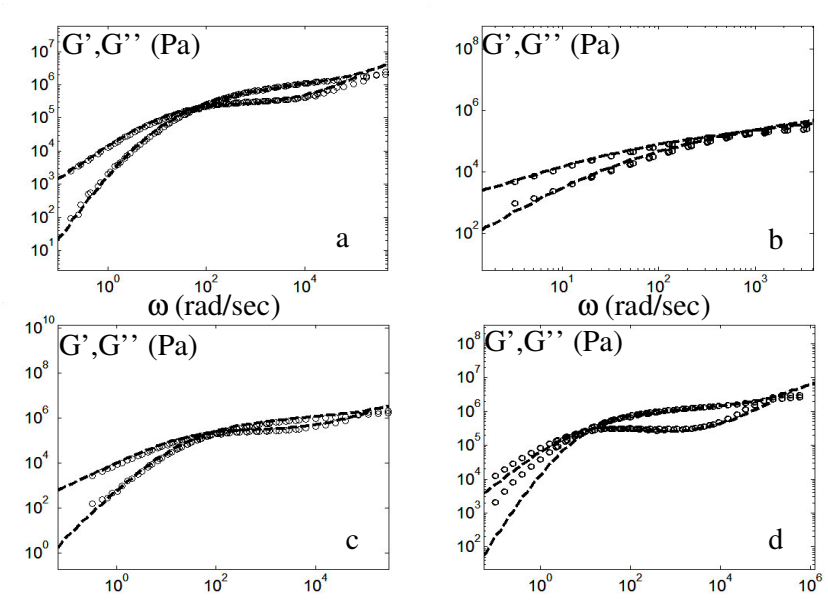

Figure 10: Comparison between experimental (oo) and theoretical (--) storage and loss moduli for a) PC1, b) PC1F1, c) PC1F2, d) PC1F3.

In this case, the branching level is too low to observe any divergence between predictions and experiments for the total sample and the lower fractions. On the other hand, the highest fraction PC1F3 clearly shows a discrepancy, which is indicative of LCB. In this case, fractionation has been a good way to enhance detection, since LCB for this sample is concentrated in the highest fraction [8]. Rheology is far more sensitive than solution characterization, which fails to detect any LCB.

6.4.3 Monte-Carlo simulations

A. Validation of the simulation by comparison with the Flory method

In order to validate our Monte-Carlo method, we have compared the simulation results for PC1 and PC2 with the same characteristics obtained by the Flory method [39]. This statistical method, which is useful for the analysis of gelation, generates the MMD of a non-linear polymeric sample and calculates the volumetric fraction of molecules containing a defined number of branching, bifiunctional and terminal units from knowledge of branching density and number average molecular weight. However, a large array of isomeric structures can be derived from these numbers and the method is unable to distinguish between "long chain" and "short chain" branches. In Fig. 11, we compare the molecular weight distributions of PC1 and PC2 measured by SEC with those calculated by the Flory and Monte-Carlo methods. Both methods use the same inputs (the values of M_n and branching density ρ; refer to Section 2)

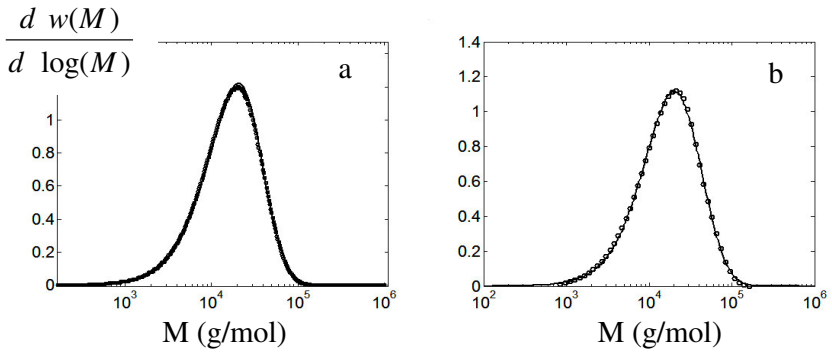

Figure 11: Comparison between SEC data (—) and molar masses distribution obtained with the Flory method (oo), for a) PC1, b) PC2.

The results obtained with both statistical methods are in perfect agreement with the distributions determined by SEC, a clear confirmation the random nature of the PC samples. In Fig. 12, the total

molar mass distributions of PC1 and PC2 obtained with the Flory and Monte-Carlo methods are compared and split in three sub-distributions: the proportion of linear chains, the fraction of star molecules (first generation tree), and the fraction of more complex molecules.

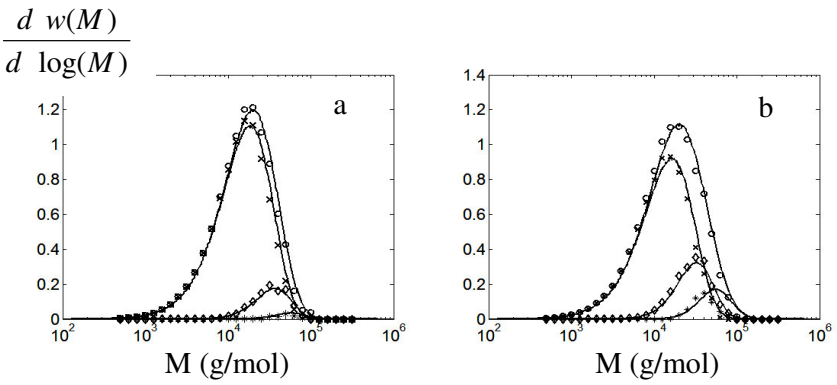

Figure 12: Comparison between the molar masses distribution obtained with the Flory method (—) and the MMD obtained with the Monte Carlo algorithm for a) PC1 and b) PC2. The total distribution (ooo) is plit in three sub-distributions: linear molecules (xxx), star molecules (◊◊) and more complex molecules (***).

Again, agreement between the two methods is very good. These results validate our simulation method, which will now essentially be used to distinguish between long and short chain branching.

B. Confrontation between simulations and solution characterisation results

Solution characterization has indicated a transition from essentially linear to slightly branched structures around 40 000 g/mol for PC2 (see Section 4.1.2). In order to extract useful information from the exhaustive architecture data resulting from the Monte-Carlo simulation, it is essential to organise the dataset by dividing the molecules into a limited number of relevant classes. In this case, we

are interested in quantifying "long chain branching" as a function of molecular weight. Therefore, we have divided the branched architectures into four categories: the linear molecules, the long chain branched star molecules, which contain three long arms, the "quasi linear" star molecules, which contain only one short chain branching, and the long chain branched molecules containing more than two branching points. Because no criterion exists to define short and long chain branching in solution, we use here, the definition of short chain branching proposed for the polymer melts [45]: an arm is considered long if it is longer than twice the molar mass between two entanglements, M_e. Furthermore, to know which chain branching is well entangled is essential to analyze the viscoelastic response of the PC.

The distribution of these different structures calculated from our simulation program is presented in Fig. 13a for sample PC2, while Fig. 13b presents the number of total and long chain branches per chain as a function of molar mass for the same sample.

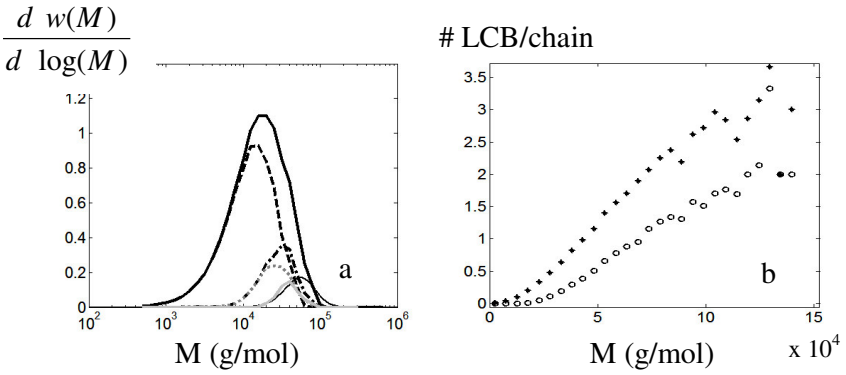

Figure 13: a) MMD obtained with the Monte Carlo algorithm for PC2. (—): total distribution, (---): linear molecules, (-·-·): star molecules, (grey ····): quiasi linear molecules, (grey —): star molecules with three long arms, (thin —): more complex molecules. b) Number of total (⁎⁎⁎) and long (ooo) chain branches per chain as a function of molar mass for PC2.

As shown in Fig. 13a by the dashed-dotted curve, star molecules appear in PC2 at a molar mass higher than 9 000 g/mol. However, these branched chains are not long arm stars, which are represented by the grey continuous curve. It seems that the short branches are not detected by SEC-viscometry. The long arm stars start appearing at 20000 g/mol, but in very small quantity. A 40 000 g/mol molar mass corresponds to approximately 0.3 - 0.5 branch per chain, as shown in Fig. 13b. This minimum value for detection of long chains branching is in agreement with the transition from quasi-linear chains to slightly branched polymers in the classification made for polystyrene blends [31]. The results obtained by our Monte-Carlo simulation are therefore in very good agreement with the observations in solution. This indicates also that the rheological definition of a long chain branch (larger than two times M_e) seems to be also convenient for solution characterization, although the origin of this coincidence is admittedly unclear. The classification of molecules for sample PC1 is represented in Fig. 14a. The number of branches per chain is described in Fig. 14b for the same sample. The concentration of molecules containing a long chain branching is really small, below the minimum detection level [5,8,31].

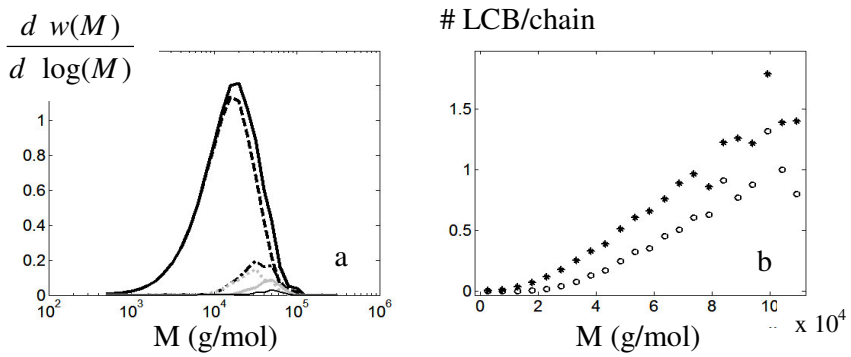

Figure 14: a) MMD obtained with the Monte Carlo algorithm for PC1. (—): total distribution, (---): linear molecules, (-·-·): star molecules, (grey ····): quiasi linear molecules, (grey —): star molecules with three long arms, (thin —): more complex molecules. b) Number of total (⁎⁎⁎) and long (ooo) chain branches per chain as a function of molar mass for PC1.

In Fig. 15, we show the local branching factor g_i for PC2, calculated by using the Zimm and Stockmayer formula [22], starting from the simulated number of total chain branches per chain. These factors are compared with the experimental g_i' determined by SEC-viscometry coupling. In this case, the curves of g and g' collapse very well in a quite large range of molar masses. Thus, no exponent in the relation ($g' = g^E$) seems useful here. In literature, models propose various values for this exponent, from 0.5 [27] to 1.5 [28], while values found experimentally go from 0.58 to 1 [25,30,63-66]. The discrepancy observed at lower masses comes from the inaccuracy of the experimental results in this region. The slightly too low value of the "plateau" observed in the experimental g_i' curve, which is theoretically equal to 1, comes from the bad superposition between experimental intrinsic viscosities of linear and branched samples (see Fig. 4). The overlap between the experimental g' curve and the theoretical g curve is an important result. Indeed, by using the Zimm-Stockmayer relation, it allows us to make directly the link between the

measured g_i' and the average number of branching units of the observed molecules.

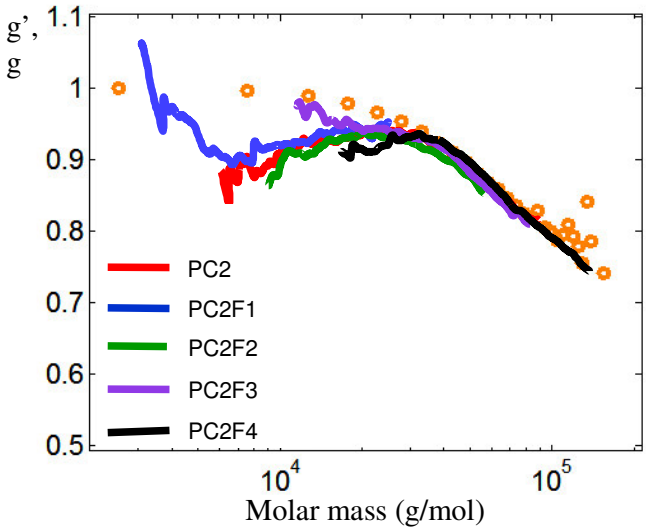

Figure 15: Evolution of g_i' with molar mass for PC2 and its fractions. (—): measured by SEC-viscometry coupling, (oo):g predicted from the Monte Carlo simulations.

C. Confrontation between simulations and rheology results

For PC2, the discrepancy between rheology predictions and experiments, which can be seen as proof of LCB, is important, in particular for the high molar mass fractions. These results are very consistent with the Monte-Carlo simulation results: PC2 and its fractions all have a significant proportion of molecules with a molar mass higher than 20000 g/mol, above which LCB appears. On the other hand, the proportion of LCB in PC1 and its fractions is very small, going from nearly zero for the lowest molar mass fraction PC1F1, to a significant proportion for the third fraction PC1F3, which is also the only fraction containing molecules with molar masses higher than 40000 g/mol. In this case, the branching density is lower

than 0.3 branching point per chain, apart from PC1F3. This last sample is the only one for which we can see a small rheological discrepancy at low frequencies.

6.5 CONCLUSIONS

We have characterized sparsely long chain branched polycarbonate and fractions of them, by using a combination of different techniques:

Solution characterization
First, solution characterization has been investigated: we obtain a global branching index in solution by comparing apparent average molar masses obtained with a linear PC specific calibration and real average molar masses obtained by universal calibration, or by looking at the global intrinsic viscosity. Next, we characterize LCB for each chromatographic slice by applying the same method, first to preparative fractions, next to blends of the fractions and finally to unfractionated samples. The lower molar mass limit for reproducible g'_i has been determined in the process. For PC2 (see Table 1), LCB effect appears for molar masses higher than 40000 g/mol. For PC1, which contains a very low level of LCB, no clear conclusion can be drawn.

Rheological characterization
Secondly, we compare the moduli of the fractionated and unfractionated samples to the predictions of a recent tube-based rheological model published by some of the authors [43]. This model is suited for blends of polydisperse linear molecules. Because the model requires the determination of three material parameters, we first calibrate it on the linear PC reference sample (PCL), and validate the calibration on three of its fractions. Keeping the same values for the material parameters, we next use the model to predict the viscoelastic behaviour of two sparsely branched PC samples (PC1 and PC2, see Table 1) and of their fractions, using the MMD obtained by SEC as input for the model and assuming that the samples are linear.

Discrepancies between predictions and experimental data give us some important indications about the presence and the level of long chain branching in PC2. For PC1 and its lowest fractions, no effect of LCB is detected. Only the highest molar mass fraction PC1F3, in which LCB are more concentrated, shows an influence of LCB on rheology. Fractionation allows thus refining this characterization technique.

Monte-Carlo simulations

Finally, we compare our results for PC1 and PC2 with the reconstructed MMD predicted from a Monte-Carlo simulation as explained above. The inputs of the simulation are the molar fraction of end-groups, obtained from the number average MW measured by SEC and the corresponding fraction of trifunctional branching points, obtained by NMR [37]. The method, as opposed to the well-known Flory approach [39], provides an exhaustive information on the shape and size of molecules across the MMD. This detailed picture can be organised by defining "classes of molecules" with significant molecular architectural features. For each class there is a corresponding MMD and this information can in turn be correlated with the solution and melt characterization results. Moreover, we determine the local branching factors g_i from simulation [22] and comare its value with experimental g_i'. Perfect overlap is found on a quite large range of masses, without using any exponent rule.

REFERENCES:

[1] F. Garbassi, *polymers News*, 19:240-346 (1994)

[2] C. Gabriel and H. Münstedt, *Rheol. Acta*, 41,232-244 (2002)

[3] P.F.W. Simon, A.H.E. Muller, T. Pakula, *Macromolecules*, 34:2677-1684 (2001)

[4] Vega, J. F., M. Fernandez, A. Santamaria, A. Munoz-Escalona and P. Lafuente, *Macromolecules*, 31, 3639-3647 (1998).

[5] Shroff, R. N. and H. Mavridis, *Macromolecules*, 32, 8454-8464 (1999).

[6] Shroff, R. N. and H. Mavridis, *Macromolecules*, 34, 7362-7367 (2001).
[7] A.M. Striegel, M.R. Krejsa, *J. Polym. Sci., Part B: Pol. Phys*., 38 :3120-3135 (2000)
[8] Gabriel, C., E. Kokko, B. Lofgren, J. Seppala and H. Munstedt, *Polymer*, 43 (24), 6383-6390 (2002).
[9] Janzen, J and R. H. Colby*, J. of Molecular Structure*, 485-486, 569-584 (1999).
[10] CY Liu, L. Chaoxu, P. Chen, J. He, Q. Fan*, Polymer*, 45:2803-2812 (2004)
[11] Crosby,B. J., M. Mangnus, W. de Groot, R. Daniels and T. C. B. McLeish, *J. Rheol*., 46(2), 401-426 (2002).
[12] Vega, J. , M. Aguilar, J. Peon, D. Pastor and J. Martinez-Salazar, *E-Polymers Art.,* 46 (2002).
[13] M.Y. Lyu, J.S. Lee, Y. Pae, *J. Applied Polym. Sci*., 80:1814-1824 (2001)
[14] Doerpinghaus, P.J., D.G.Baird, *J. Rheol.,* 47 (3), 717-736 (2003).
[15] E. van Ruymbeke, V. Stéphenne, D. Daoust, P. Godard, R. Keunings, C. Bailly, submitted in *J. Rheol*. (2005)
[16] J. de Corral, *U.S. Patent*, 5637790 (1997)
[17] Wang, W.J., S. Kharchenko, K. Migler, and S.P. Zhu, *Polymer*, 45 (19), 6495-6505(2004).
[18] J. Herz, M. Hert, C. Strazielle, *die Makromol. Chem*., 160 :213-225 (1972)
[19] P.J. Wyatt, *Anal. Chim. Acta*, 272:1-40 (1993)
[20] S. Podzimec, *J. Appl. Polym. Sci*., 54 :91-103 (1994)
[21] D. Lecacheux, J. Lesec, C. Quivoron, *J. Appl. Polym. Sci*., 27 :4867-4877 (1982)
[22] B. Zimm, W. Stockmayer, *J. Chem. Phys*., 17:1301-1314 (1949)
[23] N. Khasat, R. Pennisi, N. Hadjichristidis, *Macromolecules,* 21:1100-1106 (1998)
[24] C. Bailly, D. Daoust, R. Legras, J. Mercier, *Polymer,* 27:1410-1415 (1986)
[25] J. Douglas, J. Roovers, K. Freed, *Macromolecules*, 23:4168-4180 (1990)

[26] S.T. Balke, T.H. Mourey, D.R. Robello, T.A. Davis, A. Kraus, K. Skonieczny, *J. Appl. Sci*., 85:552-570 (2002)
[27] B. Zimm, R. Kilb, *J. Polym. Sci*., 37:19-42 (1959)
[28] W. Stockmayer, M. Fixman, *Ann. N.Y. Acad. Sci*., 57:334 (1953)
[29] D. Frater, J. Mays, C. Jackson, *J. Polym. Sci. , Part B*, 35 :141-151 (1997)
[30] N. Hadjichristidis, M. Xenidou, H. Iatrou, M. Pitsikadis, Y. Poulos, A. Averopoulos, S. Sioula, S. Paraskeva, C. Garcia-Franco, T. Sun, C. Ruff, *Macromolecules,* 33 :2424-2436 (2000)
[31] A. Kaivez, thesis
[32] M. Netopilik, P. Kratochvil, *Polymer*, 44 :3431-3436 (2003)
[33] F. Léonardi, J-C. Majesté, A. Allal, G. Marin, *J. Rheol.*, 44:675-692, 2000.
[34] A.E. Likhtman, T.C.B. McLeish, *Macromolecules*, 35:6332-6343, 2002
[35] E. van Ruymbeke, R. Keunings, V. Stéphenne, A. Hagenaars, C. Bailly, *Macromolecules*, 35(7):2689-2699, 2002.
[36] C. Pattamaprom, R.G. Larson, T.J. Van Dyke, *Rheol. Acta*, 39: 517-531, 2000.
[37] A. Hagenaars, J.J. Pesce, C. Bailly, B.A. Wolf, *Polymer*, 42 :7653-7661 (2001)
[38] A. Hagenaars, "Structural Characterization of Polycarbonate Materials across the Molecular Weight Distribution", *Thesis* (2002)
[39] P.J. Flory, *Chem. Rev*. 39:137-197 (1946)
[40] K. Shida, K. Ohno, M. Kimura, Y. Kawazoe, Y. Nakamura, *Macromolecules*, 31:2343-2348 (1998)
[41] N.C. Karayiannis, A.E. Giannousaki, V?G? Mavrantzas, I. *Chem. Phys*.,118 :2451-2454 (2003)
[42] S.Lee, J.C. Lee, H. Lee, *Polymer Journal*, "":685-689 (2001)
[43] E. van Ruymbeke, R. Keunings, C. Bailly, *J.N.N.F.M*., in press (2005)
[44] P.G. de Gennes. Reptation of a polymer chain in the presence of fixed obstacles. *J. Chem. Phys.,* 55:572-579, 1971.

[45] M. Doi, S.F. Edwards. *The theory of Polymer Dynamics*. Oxford University Press, 1986.
[46] M.J. Struglinski, W.W. Graessley, *Macromolecules*, 21, 783-789, 1988.
[47] S.J. Park, R.G. Larson, *Macromolecules*, 37: 597-604, 2004.
[48] R.H. Colby, M. Rubinstein, *Macromolecules*, 23, 2753-2757,1990.
[49] V.R. Raju, E.V. Menezes, G. Marin, W.W. Graessley, *Macromolecules*, 14, 1668-1676, 1981.
[50] S.T. Milner, T.C.B. McLeish, *Macromolecules*, 30: 2159-2166, 1997.
[51] G. Marrucci, *J. Polym. Sci., Polym. Phys.*, 23:159-177, 1985.
[52] R.C. Ball, T.C.B. McLeish. *Macromolecules*, 29:5717-5722, 1989.
[53] R.G. Larson, T. Sridhar, L.G. Leal, G.H. McKinley, A.E. Likhtman, T.C.B. McLeish*, J. Rheol*., 47, 809-818, 2003.
[54] A. Kaivez, D. Daoust, P. Godard, *Polymer*, 43 :3181-3190 (2002)
[55] A. Kaivez, thesis, chapter 2 (2004)
[56] S.T. Balke, R. Thitiratsakul, R. Lew, P. Cheung, Polym. *Mat. Sci. Eng.,* 65 :136-167 (1991)
[57] R. Bartosiewicz, C. Booth, A. Marshall, *Eur. Polym. J*., 10:783-789 (1974)
[58] A. Bastini, *Macromol. Symp*., 100 :137-142 (1995)
[59] D. Beigzadeh, J. Soares, T. Duever*, Polym. Reac. Eng*. 7: 195-205 (1999)
[60] Ferry, J.D., "Viscoelastic Properties of Polymers, 3rd Ed. (Jhon Wiley and Sons, NY, 1980.
[61] L.J. Fetters, D.J. Lhose, D. Richter, T.A. Witten, A. Zirkel, *Macromolecules*, 27, 4639-4647, 1994.
[62] CY. Liu, C. Bailly, "Fluctuation of chain inside the tube: Cross-check between the relaxation time and the relaxation modulus", submitted (2005)
[63] S. Podzimek, T. Vlcek, *J. Appl. Polym. Sci*., 82:454-460 (2001)
[64] C. Ioan, S. Ioan, B. Simionescu, J. Makromol. *Sci. Pure Appl. Chem.*, A32 : 1589-1600 (1995)

[65] J. Roovers, P. Toporowski, J. Martin, *Macromolecules,* 22:1897-1903 (1989)

[66] C. Jackson, D. Frater, J. Mays, *J. Polym. Sci., Part B*, 33:2159-2166